OTGsim: Simulation of an Off-the-Grid Radar Network with High Sensing Energy Cost

Brian C. Donovan
and David J. McLaughlin
Electrical and Computer Engineering Department
University of Massachusetts Amherst
Amherst, Massachusetts 01003
Email: bdonovan|mclaughlin@ecs.umass.edu

Michael Zink
and Jim Kurose
Computer Science Department
University of Massachusetts Amherst
Amherst, Massachusetts 01003
Email: zink|kurose@cs.umass.edu

Abstract—Many sensor network studies assume that the energy cost for sensing is negligible compared with the cost of communications or computing. Opportunities exist to deploy sensor networks utilizing active sensors with a high energy cost such as radar. For a node utilizing radar as its primary sensor, the actual sensing procedure is the main power consumer. In the worst case almost 50% of the power is consumed by the sensing procedure, while only 3% is used for communication, the remainder is consumed by the computing platform. In this paper we examine a wireless sensor network composed of short range radars used to monitor rainfall. These short-range radar nodes are designed to be deployed as part of an ad-hoc network and to limit their reliance on existing infrastructure. We refer to these networks as "Off-the-Grid" (OTG) weather radar networks. Independence of the wired infrastructure (power or communications) allows OTG networks to be deployed in specific regions where sensing needs are greatest, such as mountain valleys prone to flash-flooding, geographic regions where the infrastructure is susceptible to failure, and underdeveloped regions lacking urban infrastructure. We present a simulation based investigation of such an OTG sensor network. We focus on power management and energy harvesting for the network. We use these simulations to demonstrate how geographic location, battery capacity, optimization of power consumption, and node density have an impact on the performance and operational lifetime of such a sensor network. In addition to these simulations, we present the design and implementation of an OTG prototype sensor node. Experiences and data gained from the operation of this node are used as input parameters for the simulations.

I. Introduction

It has been shown that the combination of power management and energy harvesting can significantly extend the lifetime of wireless sensor networks. Recently, research in the area of power management and energy harvesting has been focused on small, low-power, sensor systems where data communication is the main power consumer. In this paper, we focus on power management and energy harvesting for a sensor system where the actual sensing procedure is the main power consumer. In the worst case almost 50% of the power is consumed by the sensing procedure, while only 3% is used for communication, the remainder is consumed by the computing platform.

In our specific case we are investigating radar sensor networks with the intent to improve severe weather observations. Such radar sensor networks have the potential to improve our ability to observe, understand, forecast, and respond to weather hazards. These Distributed Collaborative Adaptive Sensing (DCAS) networks will map wind, rain, and thermodynamic variables in the lower troposphere and provide real-time data to end users [1]. Our work is an extension of the existing DCAS concept by introducing a minimal infrastructure architecture. Minimal infrastructure in this case means sensor nodes that operate without gridded power and wired network access [2]. Such Off-the-Grid characteristics are extremely important in the case of radar sensors, since the location of the sensor has a high impact on the quality of the sensed data. For example, mountains can block the radar beam and prevent the lower atmosphere in valleys behind mountain ranges from being sensed. Sensor nodes that are independent of existing infrastructure can be placed in more optimal locations to prevent the phenomena of radar beam blockage as described above. The price for this location independence is to enable these sensor nodes with energy harvesting and wireless communication means that allow the maximization of their operational lifetime.

In this paper, we present a simulative investigation of such an OTG sensor network. We use these simulations to demonstrate how geographic location, battery capacity, optimization of power consumption, and node density have an impact on the performance and operational lifetime of such a sensor network. In addition to these simulations, we present the design and implementation of an OTG prototype sensor node. Experiences and data gained from the operation of this node are used as input parameters for the simulations.

Results obtained from these simulations show that the design of such a sensor network is highly dependent on its geographical location. In addition, we show that a reduction in space between sensor nodes (while the size of the overall deployment area is kept constant), surprisingly, leads to lower battery levels. Finally, we believe that OTGsim is the first modular sensor network simulator that allows for an easy exchange of components composing the sensor node due to its sub-model design approach.

The remainder of the paper is organized as follows. In Section II we give an overview on the related work in the area of power management and energy harvesting. The OTG radar

sensor network concept including a description of the radar sensor prototype is presented in Section III. Section IV gives an overview on the simulator that was created to simulate such a wireless sensor network. The results of a series of extensive simulations are presented in Section V. Finally, we conclude the paper and give an outlook on future work in Section VI.

II. Related Work

This work expands upon simulation results initially reported in [3]. Related work in power management in sensor networks may be divided into two categories. The first category, contains work on energy-aware protocols that are solely based on battery level and do not take energy harvesting into account. For example, Wang et al. [4] develop an energy consumption model for wireless sensor networks. Compared to our approach, their model is only focused on the communication subsystem and does not consider power consumption of other components (e.g., sensing and computing) of a sensor node.

The second category, which is more strongly related to our work, is focused on systems that incorporate energy harvesting as an additional power supply [5], [6]. Raghutan et al. [5] identify tradeoffs for the design of a solar energy harvesting module and show the difference of battery-only systems. This investigation leads to design consideration for energy harvesting systems, which are evaluated on the Heliomote system. In contrast to our work, their work is focused on low power embedded systems that consume power in the order of mW. In [7], the authors extend their work on energy harvesting by an algorithm that adapts the duty cycle of a node based on the input of a periodic harvested energy source (e.g., solar power). Vigorito et al. [6] developed an adaptive control of duty cycling for energy-harvesting wireless sensor networks that does not require a model to predict future harvested energy but simply operates on the actual battery level. The adaptive control approach is evaluated by a single sensor node simulation.

Our work is different in a sense that we do not adapt duty cycling to available energy. The goal in this initial investigation is to study the performance of a specific wireless sensor network in different configurations. For example, we determine the maximum possible duty cycling frequency based on available energy and geographic location. In future work, we plan on implementing the adaptive control mechanism presented in [6] into our sensor nodes to investigate if the duty cycling frequency of the single nodes can be increased.

The deployment of radar as a network of collaborative instruments was introduced by McLaughlin et al. [1]. This work focused on introducing collaborative sensing to the radar sensing paradigm. Pedersen et al. [8] have deployed marine radars as short range weather radar. Our work extends that of [1] and [8] by introducing sensor network concepts such as energy harvesting and wireless networking.

III. OTG Radar Sensor Network

A. Concept

The Off-The-Grid (OTG) radar class combines wireless sensor networks [5], [9]–[11] with the DCAS concept [1]. By employing wireless sensor network techniques such as ad-hoc networking, energy harvesting and dynamic management, an OTG network minimizes its dependence on existing infrastructure.

Utilizing these three techniques, an OTG radar node has the capability to: (a) source its prime power needs using energy harvesting rather than existing power infrastructure, (b) transport its data and control communications via a wireless long-distance communications network rather than existing network communication infrastructure, and (c) manage its energy consumption by adapting its functionality to the environmental conditions.

Power is consumed within the radar node by three functions of the node: sensing, computing, and communicating. Maximizing the lifetime of the sensor network, perhaps at the expense of an individual node, will require balancing trade-offs between these three functions. Appropriate design of energy aware control algorithms may take advantage of both prior knowledge of the target application and environment as well as dynamic knowledge of the operating environment.

B. Radar Node

We developed an OTG radar prototype to provide a demonstration of an OTG class node, to inform simulations of an OTG network, and to provide a platform for experimentation. The experience gained using the node and measurements of its performance have been used to model the network scale simulation of an OTG system. This is presented in Section IV. This section will document the prototype which has been developed and deployed.

Figure 1 presents a block diagram of the general hardware architecture of the prototype node. The four major subcomponents of the system are: the solar power generation, computing, radar, and communication subsystems. The solar power generation subsystem is composed of a 60W ($\sim$ 0.5 m^2) solar panel, a maximum power point tracker (MPPT), a deep-cycle battery, and a battery charger. The computing subsystem uses a low power x86 embedded computer and integrates with the sensing subsystem using a PCI analog to digital converter (ADC) and a custom, USB based, control interface. The sensing subsystem is composed of a commercial marine radar which has been modified to allow for integration with the remainder of the system. The communication system uses a PCMCIA 802.11b/g (WiFi) wireless card and an external directional antenna to provide communications between nodes [12]. Figure 2 shows a picture of the fully integrated prototype node. The electronics box contains all components excluding: the radar, solar panel, battery and WiFi antenna. The contents of the electronics box is shown in Figure 3.

The node is built around a 12 V power bus provided by the MPPT. The MPPT regulates power generation from the solar
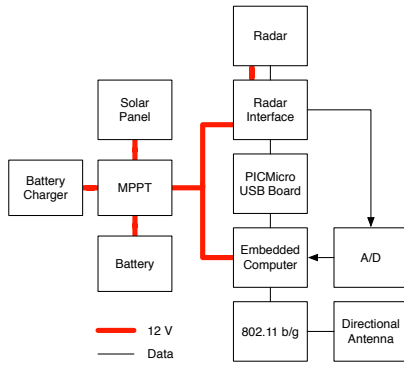
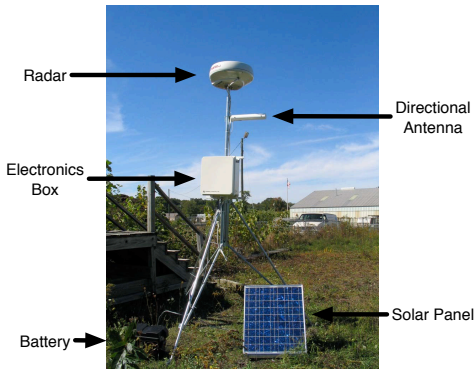Fig. 1.   OTG prototype hardware architecture.

Fig. 2.   OTG prototype node.

Fig. 3.   OTG prototype electronics box.

Sensing		Computation		Node	
Heater / Controller	10	Motherboard	17	Sensing	34
Motor / Inefficiencies	21	A/D	13	Computation	33
Avg. Radiated Power	3	Storage	3	Comm.	2
Total	34	Total	33	Total	69

rotating and the magnetron is firing (producing the pulses of energy used for sensing).

In addition to the radar, power will be consumed by the computation and communication functions of the OTG node. The computation function is composed by three main components: the motherboard, the PCI ADC card, and a compact flash card. The power consumption for computation is comparable to that of the sensing function. If the sensing function is not being used the ADC would not be required, reducing the power consumption of the computation system by 40%.

The final function of an OTG node is the communications function. The OTG prototype uses 802.11b/g for point-to-point wireless communications. A PCMCIA wireless card is paired with a passive directional antenna in order to achieve long distance communications (5-30 km). The wireless card currently being used draws approximately 2W when transmitting and 1.4W when receiving [12].

Table I presents the empirical worst-case power consumption of each of the three functions of the node. This data in this table was measured at the 12 V bus supplying the complete node. The power consumption was measured as each function was enabled.

IV. OTG SIMULATOR

We have developed a network simulator, *OTGsim*, to study potential OTG networks. OTGsim is a discrete time simulator that models networks of OTG nodes and their communications. Simulation of OTG networks enables experimentation with the OTG concept without the expense of a full OTG network deployment. Networks of tens to hundreds of OTG nodes may be simulated to study the impact of: network location, node spacing, data routing, and control decisions. Simultaneously, the deployment of small scale OTG networks will enable the validation and refinement of the OTG simulator. We are currently in the process of deploying a 3-node OTG testbed in Western Massachusetts to validate the simulation results presented in this paper.

The OTG simulator focuses on the the radar sensor and energy harvesting portions of an OTG network. The aim of the simulator is to complement existing networking simulators such as ns-2 [13] and integrate their output to simulate the communications portion of the simulation.

The OTG simulator provides a general framework which may be developed to extend the models to other high-energy sensor types. Modules of the simulator may be replaced individually to study alternative control schemes, sensor systems (LIDAR or more advanced RADAR) and power generation. In

panel and storage in the battery. The battery charger is included to charge the battery or provide 12 V when infrastructure power is available[1]. The 12 V bus powers both the embedded PC and the radar. The radar is powered through the USB interface card which allows the radar power to be switched under computer control.

C. Power Consumption

This section presents the power breakdown for the major functions of the OTG prototype.

Power is consumed in the radar by the electronics required to control the radar, the motor rotating the antenna and the high power pulse generating magnetron. In standby mode the electronics and magnetron heater are active while the antenna is not rotating. When the radar is transmitting the antenna is

[1]This way the radar can be powered via regular 110V gridded power for hardware debugging in the lab.

this paper, the OTGsim is used to study networks composed of nodes similar to the OTG prototype described in Section III-B.

A. OTG Network Simulator

The OTG simulator is built using the SimPy discrete simulation package [14]. During a simulation run a network topology consisting of one or more nodes is created. Every node is composed of sub-models for each of the four subsystems: sensing, computing, communicating and power generation. The sub-models report their energy consumption or generation to an energy aware control module. A network definition file is used to describe the node's locations and the network links between nodes.

Two external data sources are used to drive the simulations. The U.S. National Renewable Energy Laboratory's Typical Meteorological Year 2 (TMY2) data set [15] is used to drive the estimation of solar power generation. In addition, radar data (NEXRAD) from the National Climatic Data Center Data Archive [16] is used to simulate "workloads" for the network. The archive data may be used to simulate the data that each radar in the network would observe. This may be used to evaluate dynamic control, network routing and data compression algorithms specific to the weather radar application.

The power sub-model models a fixed tilt solar panel of a specified area. The solar power incident on the panel is estimated from the TMY2 data set using the procedure described in [12]. The effect of panel tilt, area, efficiency and snow cover are included in the estimation. Simplified, the estimated power output of the panel is,

$$P = eI_T = eI(\theta, \beta, \rho_g, t) \tag{1}$$

where P is the power generated by the panel, e the efficiency of the panel, and I_T the total radiation incident on the panel. The total radiation incident on the panel is a function of the panel's latitude (θ), tilt (β), the reflectance of the ground (ρ_g) as estimated by the snow cover, and the solar time t. In these simulations the solar panel was vertically tilted at an angle equal to the latitude of the node and facing due south, the power optimal directions for a fixed tilt solar panel in the northern hemisphere [17]. If a NEXRAD data set is used to drive the simulation the incident solar power is set to zero if there is positive reflectivity (indicative of rain) in the node's coverage area. Power generated by the panel is stored in the battery model.

The computation sub-component generates tasks for the energy aware control to select from. It also includes both the radar control and network routing algorithms. The radar control issues *radar scan* tasks which may be generated at fixed time intervals or based on the weather environment. Different control schemes may be tested by replacing this module. The network routing control implements the distance vector routing algorithm (DVR) [18] to create network routes for each node. In this paper the DVR algorithm uses the physical node separation as the distance metric for the calculation of

the networking routes. Alternatively the simulator may use a metric based on the node battery level. Future simulation will study the utility of applying existing energy based sensor network routing algorithms. A key question to examine is the impact that high sensor power consumption may have on the metrics used in routing decisions.

The networking model simulates a simplified networking stack. It assumes: (a) a reliable networking paradigm where messages may be passed between nodes, and (b) a physical link provided by 802.11 b/g hardware operating at the maximum fixed speed, 8 Mbps, observed in simulated tests [19]. Energy consumption is estimated on a per message basis based on message size (in bytes), the transfer speed and the energy consumption of the networking card. Transfers proceed if both the sender and the receiver have sufficient energy, otherwise the message is buffered at the sender. For the simulations we assume an unlimited buffer. OTGsim currently simulates at the level of individual messages and does not implement the full networking stack including the MAC or physical layers. Future improvement to the networking component will include integration of ns-2 wireless simulation.

The radar model estimates the energy consumption required to sample the atmosphere. The energy consumption is estimated from the total transmit time of the scanner and the energy consumption rate of the transmitter. If NEXRAD data is available the data is "sampled" to an azimuth-range array based on the beamwidth characteristics of the simulated antenna. The sampled data is then passed to energy aware control for further computation or transmission. The default scan pattern is a 360° azimuth scan at 0° elevation over 30 seconds.

B. Network Topology Generator

The OTG networks used in the following experiments are generated automatically from user defined seed sites[2] using a desired range between nodes. Line of sight between nodes is estimated using United States Geological Survey (USGS) 1° Digital Elevation Maps [20] to determine communication links between nodes. Nodes are added to the network in multiple rounds. Starting from the each existing node (seed nodes in first round), potential locations are generated around the node in a circle with the desired radius. Potential nodes are eliminated by limiting overlap with existing nodes to the desired range and requiring a line-of-sight to at least one existing node. The remaining nodes are filtered to maximize distance and the number of line-of-sight links between nodes. The nodes that remain after filtering are added to the network and the process repeats until the user-defined area has been covered. The result is a fully connected network of nodes satisfying line-of-sight communications (excluding trees, man made structures, and the effect of the fresnel zone).

Figure 4 illustrates six potential OTG network deployments generated using the above procedure. The figure indicates

---

[2]For example, a seed site could be a location with wired infrastructure serving as a gateway between the sensor network and the Internet.

(a) 5 km spacing, 239 nodes   (b) 10 km spacing, 60 nodes   (c) 15 km spacing, 24 nodes

(d) 20 km spacing, 17 nodes   (e) 25 km spacing, 10 nodes   (f) 30 km spacing, 8 nodes
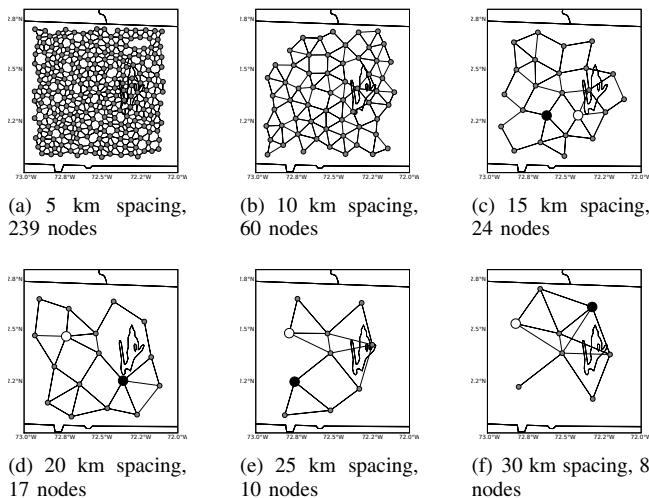
Fig. 4. Example networks for simulation. Dots indicate node location. White and black dots indicate nodes with minimum and maximum cumulative battery level as discussed in Section V-D. Black lines indicate line of site communications link. Domain is located in Western Massachusetts. The outlined shape in the maps is the Quabbin Reservoir near Belchertown, MA.

the locations of nodes in the network and the line-of-sight communication links between nodes. These networks were generated based on the terrain in Western Massachusetts near the University of Massachusetts Amherst. Networks were generated for ranges from 5 to 30 km spacing. The longer ranges are limited by the line of sight requirement which prevents coverage in some locations.

These hypothetical networks have been used to simulate OTG network performance.

V. SIMULATIONS

We performed a number of experiments using the OTG simulator to explore the performance of an OTG sensor network as it is described in Section III. The primary metric examined in this paper is the battery level of the individual nodes. If the battery level drops to 0% the node will fail due to lack of power. All of these experiments were simulated with a 60 second time resolution.

In this section we present the result of a number of simulation experiments using the OTG simulator. In Section V-A we present the variation in generated power due to the geographic location of the network. Section V-B evaluates the impact of the solar panel and battery on extending lifetime performance. Section V-C considers the potential power optimization of the sensing and computing platforms composing the node. Finally, in Section V-D we evaluate the impact of node separation.

A. Geographical Location

The first experiment examines the impact of the variation in solar input due to geography. In this experiment OTG nodes were simulated in 6 locations (as shown in Figure 5) across the United States and Puerto Rico. The goal of this experiment is to show how much energy can be created by a single OTG node based on its geographical location.
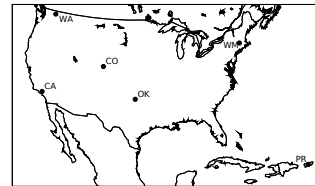

Fig. 5. Location of the different geographical sites chosen for the simulation experiment.

In this simulation an OTG node is outfitted with a southward facing 0.5 m^2 solar panel tilted at an angle equal to the latitude of the node. Each location was simulated for 18 months with an empty battery[3] at the initialization of the simulation. Daily solar generation for each of the six sites is shown in the top subfigures of Figure 6 in Watt-hours (Wh) for the 18 month period. The estimated solar power is based on the TMY2 data set with an assumed panel efficiency of 14%.

In general, the peak daily solar power generation for all six sites is between 500 and 600 Wh. The minimum daily generation falls below 100 Wh for the northern sites (WA and WM) while the more southerly sites have more narrow ranges between minimum and maximum generation. The trend in generated solar power becomes more apparent when the mean daily solar generation is averaged to monthly intervals, as shown in the bottom subfigures of Figure 6. The northerly sites (WM,WA) suffer from severe reduction in available power during winter months. This limits the ability of such sensor networks to survive during winter months. A functioning radar sensor network at these locations is crucial due to the threat of winter storms.

B. Battery & Panel Area

In this simulation, the nodes making up the networks are based on the prototype described in Section III-B. It is considered that the radars operate in a fixed interval scan pattern. That means, the radar scans its volume for 30 seconds and then "sleeps" for 5, 10 or 15 minutes. We assume that the radar does not draw any power while sleeping and does not require any time to wake from sleep. This assumption neglects the boot time and energy draw during times when the CPU is not active but the memory continues to draw power. Therefore, the results presented here may be considered the best case scenario for power consumption.

We also assume that the radar node can be woken up via remote signaling over the wireless network if sufficient power is available at the node. In the following, we study the performance of an OTG radar sensor network based on battery level. We use the battery as a performance measure, since it indicates when a node can operate and when not. Thus, the battery level can be used as a measure to compare the performance of different configurations (e.g., different routing

[3]Since we were interested in the ramp up behavior of the system with a completely depleted battery, we started the simulations with an empty battery. In an actual deployment nodes would be initially installed with a fully charged battery
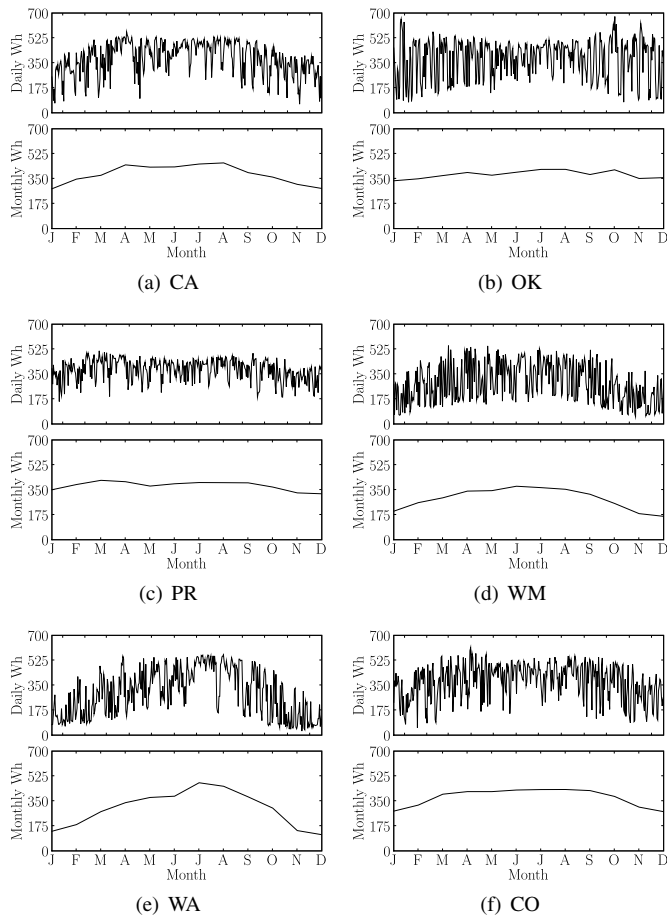
Fig. 6. Daily and monthly mean estimated solar power generation in Wh for the six sites in the location experiment.

Fig. 7. Battery level in percentage capacity relative to a 110 Ah battery. Nodes were simulated with an unlimited battery, 0.5 m^2 panel and three different scan interval times: 5, 10 and 15 minutes.

mechanisms) of the OTG network at different locations. For this simulation two battery scenarios were considered: (1) the battery had infinite capacity, and (2) the battery capacity was limited to 110 Ah. In each case the battery was completely empty at the beginning of the simulation. For both simulations we assume radar networks with a 30 km node spacing. An example network topology for the Western Massachusetts location is shown in Figure 4(f). Data created at the nodes is forwarded - according to routes determined by the distance vector routing protocol - to the seed site at the center of the network, which represents the data sink.

1) Unlimited Battery: During the first experiment the battery associated with each node was allowed to store an unlimited amount of energy. In this scenario, it is possible to determine if the node is limited by the solar power generated or if it is limited by the battery's capacity. Figure 7 presents the battery level at each site for the 5, 10 and 15 minute sleeping times of the radar. The battery level is presented in units of percent capacity of a 110 Ah battery. This is the same battery size used in the prototype and in the limited battery experiment (see Section V-B2).

Figure 7 indicates that all of the six locations are capable of supporting year round operation for each of the three scan
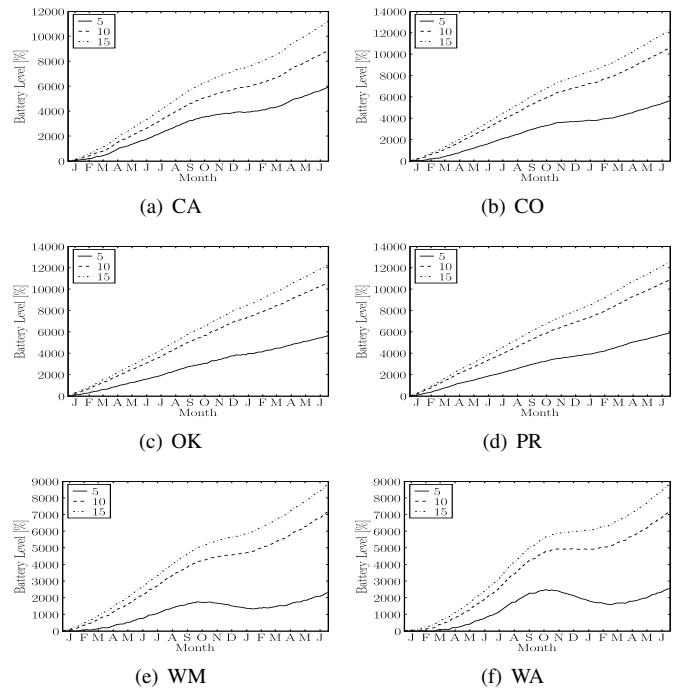
intervals if an unlimited capacity battery is used. This is indicated by the fact that none of the battery levels returns to 0 after the start of the simulation. Figures 7(e) and 7(f) demonstrate that a large battery will be required for these two locations to buffer the energy loss during the months from October to January where the battery level dips as more power is consumed than is generated.

Figure 8 presents a second unlimited battery experiment in which the panel size was reduced for the Western Massachusetts (WM) and Washington state (WA) sites. Reducing the solar panel in size has an beneficial impact on cost and wind loading. Especially the latter is of importance if a node is installed on smaller tower structures like the tripod shown in Figure 2. In this experiment the battery is again unlimited and the panel size is simulated with 0.375, 0.438 and 0.466 m^2 areas while the scan interval remains fixed at 5 minutes. As the figure indicates both locations are unable to support a 5 minute scan interval if the panel is reduced to 0.375 m^2.

In the following we take a look at the combination of panel size, load, and available solar input power to determine the required battery capacity. The size of the required battery may be determined from the capacity difference between the two inflection points in each line of Figure 8. For example, for nodes in WA using a 0.438 m^2 panel the battery charge peeks at approximately 1500% and drops to 500% relative to a 110 Ah battery. Therefore a battery with a capacity 10 times the prototype battery, or approximately 1100 Ah would be required to operate the node year round. As the panel size is increased the required battery size is reduced as more energy is produced during the low energy months. For WA a node
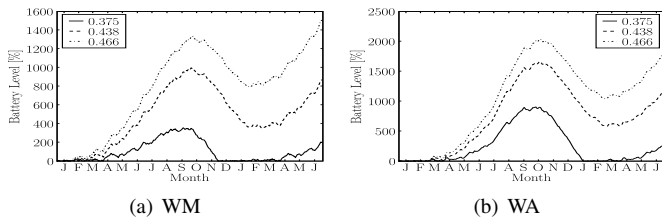
(a) WM

(b) WA

Fig. 8. Battery level in percentage capacity relative to a 110 Ah battery. Nodes were simulated with an unlimited battery using a 5 minute scan interval at four different panel sizes 0.500, 0.531, 0.563 and 0.625 m^2.

with a 0.5 m^2 panel would require a battery of approximately 900 Ah. Batteries this large, while possible, are unrealistic for a sensor network deployment because of their high cost and weight.

2) Limited Battery: In the limited battery experiments the battery capacity of the node is limited to 110 Ah. Like the unlimited battery experiments the radars use a fixed interval scan time with a 30 second scan followed by a fixed sleep time of 5, 10 or 15 minutes. Figure 9 presents the battery level over 18 months using the same networks and locations as the unlimited battery experiments. In this experiment the battery constrained networks are WM and WA. In these two locations the nodes were unable to support the 5 minute scan interval. The WM site did not generate enough energy to scan between November and mid January while the WA site could not scan between November and mid February. WM and WA were both able to support 10 and 15 minute interval scans year round. The other four sites support all three scan intervals year round.

For the battery limited sites increasing the solar panel or the battery will reduce the time during which the node is unable to scan. Figure 10 shows the results of a second limited battery experiment in which the panel and battery size was increased for both the WM and WA sites while the radar scanned every 5 minutes. In this experiment six combinations of panel (0.4, 0.5 or 0.6m^2) and battery (110 or 220 Ah) were simulated. For the WM site each additional tenth of a meter squared of solar panel extended the operation time by an additional month. When combined with a 220 Ah battery and a 0.6 m^2 panel the WM site was able to support 5 minute scan intervals. Adjusting panel and battery size had a more limited impact on the WA site. A 220 Ah battery and a 0.6 m^2 panel extended operation by approximately a month but was unable to support full 5 minute scans year round.

C. Optimizing Power Consumption

In addition to increasing the available power by adjusting panel size or battery capacity, node operation time may be extended by reducing the power consumption of the various subsystems. In this experiment the power consumption of the computer and radar were reduced to examine the potential to increase node operation time. Each node was simulated with a 0.5 m^2 panel and a 110 Ah battery. The computer and radar power consumption was varied independently. Each node was
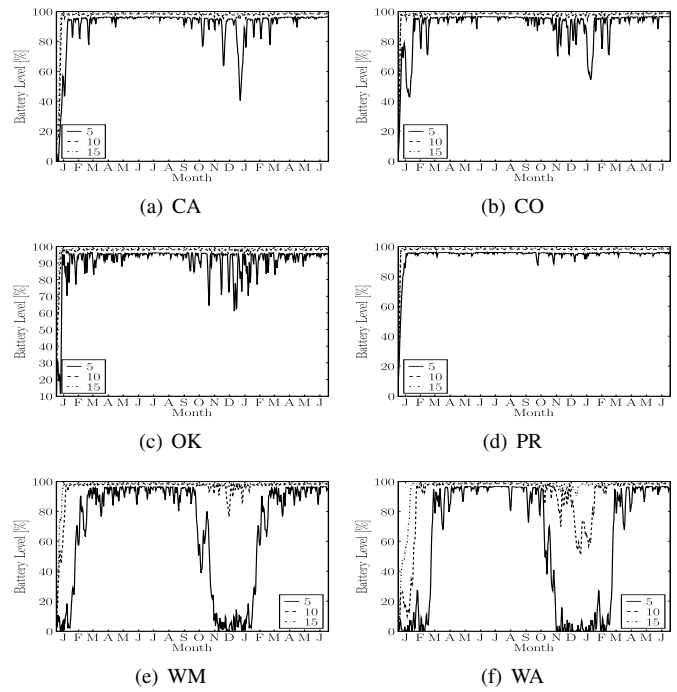

(a) CA

(b) CO

(c) OK

(d) PR

(e) WM

(f) WA

Fig. 9. Battery level in percentage capacity relative to a 110 Ah battery for six locations with a fixed 110 Ah battery capacity.

(a) WM 0.4 m^2

(b) WA 0.4 m^2

(c) WM 0.5 m^2

(d) WA 0.5 m^2
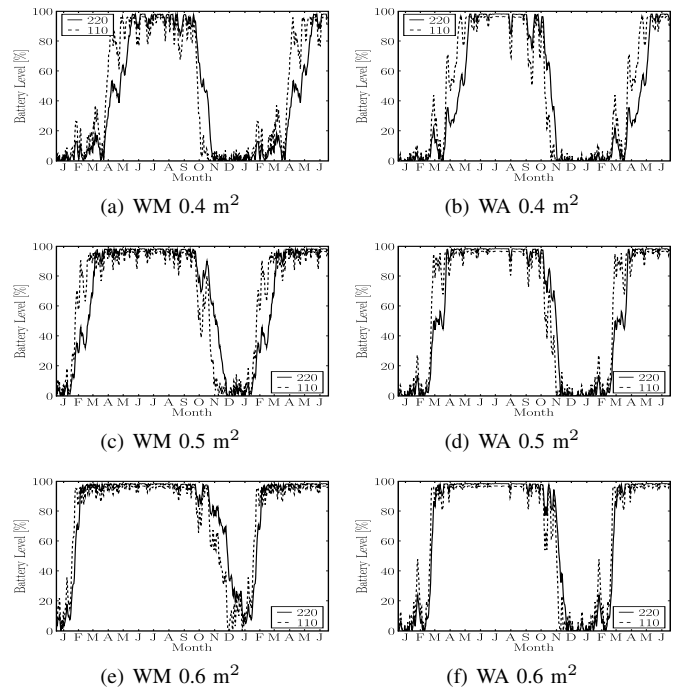
(e) WM 0.6 m^2

(f) WA 0.6 m^2

Fig. 10. Battery level in percentage capacity for two locations each with two battery capacities and three solar panel areas. Battery capacity is presented in percent capacity relative to the battery size (110 or 220 Ah). Panel size is 0.4, 0.5 or 0.6 m^2.

simulated with a 5 and 10 Watt reduction from the prototype's power consumption for each sub-system. The nodes used a 5 minute scan interval. The WM site was used for the simulation.

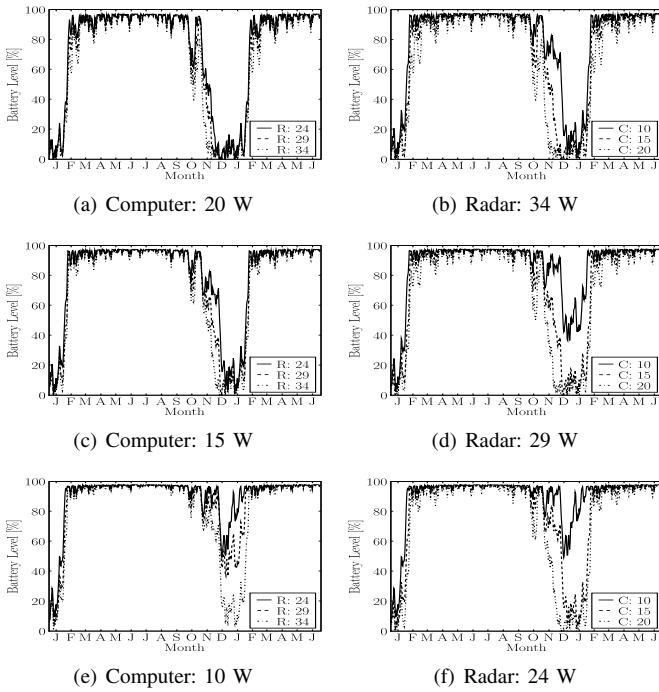Figure 11 presents the battery level for the reduced con-

(a) Computer: 20 W

(b) Radar: 34 W

(c) Computer: 15 W

(d) Radar: 29 W

(e) Computer: 10 W

(f) Radar: 24 W

Fig. 11. Battery level in percentage capacity relative to a 110 Ah battery for 9 different system configurations.
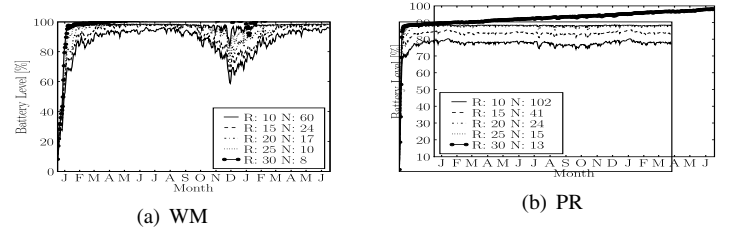

(a) WM

(b) PR

Fig. 12. Average battery level for WM and PR, node separation was been varied from 10 - 30 km. The number of nodes in each network is indicated in the legend of the figure.

sumption systems. In the left column the computer power consumption is fixed while the radar power consumption is varied. In the right hand column the radar power consumption is fixed while the computer consumption is varied. The experiment indicates that reducing the computer consumption has a greater effect on the operation time than the reduction of radar consumption. This is likely due to the greater amount of time that the computer operates as it is on during network operations (transmitting and forwarding data) as well as during the sensing periods.

D. Node Separation

The node spacing experiment examines the impact that separation has on energy consumption. Networks were simulated in two locations, WM, and PR, using separations of 15, 20, 25 and 30 km (example networks for different separation distances for the WM site are shown in Figure 4). The coverage area of the network is fixed. As the separation decreases the total number of nodes in the network increases. The range of the radar at each node is set equal to the node spacing. While this implies that each node produces less data, overlap in areas that are scanned by multiple radars may increase thereby increasing the total amount of data collected [12]. Increased overlap with smaller node spacing is caused by an increase in the number of points which may be sampled by more than one radar as the spacial density of the radars is increased.

Figure 12 presents the average battery level across all of the nodes in the network. The reduction in range resulted in lower battery levels. As the range is reduced the number of hops and therefore number of network transmissions required

to pass data through the network increases. The reduction in range does not result in power savings in the sensing function as the power consumption for that function is fixed by the transmitter type.

The impact of network activity is illustrated by comparing the nodes with the maximum and minimum battery levels over the 18 month period. Figure 13 shows the nodes with the maximum and minimum battery levels for each of the networks while Figure 14 shows the total network traffic for those same nodes. These nodes for the WM case are indicated by the black and white dots in Figure 4. In most cases the node with the minimum battery was one hop from the sink node which was in the center of the network. While the nodes with the maximum battery was located on the edge of the network. This suggests that the energy hotspot is being caused by the forwarding of data for other nodes, following the funneling effect [21].

The nodes with minimum battery level processed significantly more data than the nodes which had the maximum battery levels. While the power consumption of the networking is small compared to the other components the power consumed by the associated computing causes significant energy consumption. Figure 13 demonstrates that network activity may cause some nodes to fail. The battery level of some nodes in the network reaches 0% of capacity at which point the node fails due to lack of power. In future work, we plan to integrate an approach for joint sensing and routing developed by Chun et al. [22].

VI. CONCLUSION

The combination of power management and energy harvesting can significantly increase the lifetime of individual sensor nodes and the sensor network these sensor nodes constitute. In this paper, we look at the special case of an Off-the-Grid sensor network where the actual sensing procedure is the main power consumer. We present the prototype design of a sensor node for such a network and report the energy consumption of the node's components. In addition, we present a simulator (OTGsim) that allows the simulation of OTG sensor networks to analyze certain characteristics of such kinds of sensor networks. Subsequently, we analyze some of these characteristics via simulations that are based on the OTGsim simulator. Results of these simulations show that: (a) the geographical location of a network has an impact on its
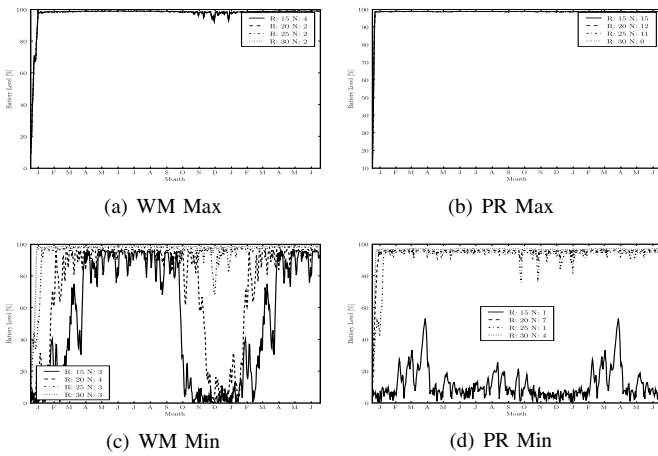
(a) WM Max (b) PR Max

(c) WM Min (d) PR Min

Fig. 13. Battery level of the nodes with the maximum and minimum cumulative sum battery levels.

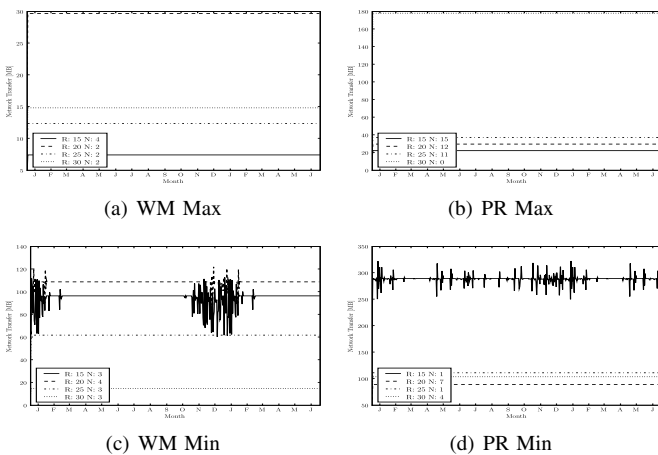
(a) WM Max (b) PR Max

(c) WM Min (d) PR Min

Fig. 14. Sum total network traffic, send and receive, of the nodes with maximum and minimum cumulative sum battery levels identified in Fig. 13.

performance; (b) increased node density does not necessarily increase the network's performance; (c) different components (radar, computer) can have an impact on the networks lifetime.

We have started deploying OTG nodes in Western Massachusetts and are in the process of collecting power management information from these nodes. The USB interface board in the prototype has been modified to allow for online monitoring of the current draw to each of the node's subcomponents. After having collected sufficient information from the testbed we will compare these results with the simulation results presented in this paper.

REFERENCES

[1] D. J. McLaughlin, V. Chandrasekar, K. Droegemeier, S. Fraiser, J. Kurose, F. Junyent, B. Philips, S. Cruz-Pol, and J. Kurose, "Distributed Collaborative Adaptive Sensing (DCAS) for Improved Detection, Understanding, and Predicting of Atmospheric Hazards," in *Ninth Symposium on Integrated Observing and Assimilation Systems for the Atmosphere, Oceans, and Land Surface*. San Diego, CA: AMS, 2005.

[2] B. C. Donovan, D. J. McLaughlin, V. Chandrasekar, and J. Kurose, "Principles and Design Considerations for Short-Range Energy Balanced Radar Networks," in *International Geoscience and Remote Sensing Symposium*, Seoul, Korea, 2005.

[3] B. C. Donovan, D. J. McLaughlin, M. Zink, and J. Kurose, "Simulation of minimal infrastructure short-range radar netowrks," in *International Geoscience and Remote Sensing Symposium*, Barcelona, Spain, 2007.

[4] Q. Wang and W. Yang, "Energy Consumption Model for Power Management in Wireless Sensor Networks," in *Proceedings of the IEEE SECON Conference, San Diego, CA, USA*, June 2007.

[5] V. Raghunathan, A. Kansal, J. Hsu, J. Friedman, and M. Srivastava, "Design considerations for solar energy harvesting wireless embedded systems," in *IEEE International Conference on Information Processing in Sensor Networks*, April 2005.

[6] C. M. Vigorito, D. Ganesan, and A. G. Barto, "Adaptive Control of Duty Cycling in Energy-Harvesting Wireless Sensor Networks," in *Proceedings of the IEEE SECON Conference, San Diego, CA, USA*, June 2007.

[7] A. Kansal, J. Hsu, S. Zahedi, and M. B. Srivastava, "Power management in energy harvesting sensor networks," *ACM Transactions on Embedded Computing Systems*, vol. 6, no. 4, Sept. 2007.

[8] L. Pedersen, N. E. Jensen, and H. Madsen, "Network architecture for small x-band weather radars - test bed for automatic inter-calibration and nowcasting," in *33rd AMS Conference on Radar Meteorology*, August 2007.

[9] G. J. Pottie and W. J. Kaiser, "Wireless integrated network sensors," *Communications of the ACM*, vol. 43, no. 5, pp. 51–58, May 2000.

[10] C. Chong and S. Kumar, "Sensor networks: evolution, opportunities, and challenges," *Proceedings of the IEEE*, vol. 91, no. 8, August 2003, DOI: 10.1109/JPROC.2003.814918.

[11] K. Romer and F. Mattern, "The design space of wireless sensor networks," *IEEE Wireless Communications*, vol. 11, no. 6, pp. 54–61, Dec 2004.

[12] B. C. Donovan, D. J. McLaughlin, M. Zink, and J. Kurose, "Design and simulation of minimal infrastructure short-range radar networks," University of Massachusetts, Tech. Rep. CMPSCI-2007-061, Nov. 2007.

[13] *The Network Simulator*, USC / ISI, http://www.isi.edu/nsnam/ns, Cited: December 7, 2006.

[14] *Simulation in Python*, SimPy Developer Team, http://simpy.sourceforge. net/, Cited: September 25, 2007.

[15] W. Marion and W. Urban, *User's Manual for TMY2s*, http://rredc.nrel. gov/solar/old_data/nsrdb/tmy2/, 1995, Cited: April 27, 2007.

[16] *NCDC NEXRAD Data Inventory*, U.S. Department of Commerce, National Climatic Data Center, http://www.ncdc.noaa.gov/nexradinv/, Cited: September 20, 2007.

[17] J. A. Duffie and W. A. Beckman, *Solar Engineering of Thermal Processes*, 2nd ed. New York, NY: Wiley-Interscience, 1991.

[18] J. F. Kurose and K. W. Ross, *Computer Networking: a top-down approach featuring the Internet*, 2nd ed. Boston, MA: Addison-Wesley, 2003.

[19] R. Patra, S. Nedevschi, S. Surana, A. Seth, L. Submaramanian, and E. Brewer, "Wildnet: Design and implementation of high performance wifi based long distance networks," in *Proceedings of the USENIX NSDI conference, Cambridge, MA, USA*, Apr. 2007.

[20] *USGS 1:250,000 DEM FTP Archive*, U.S. Department of the Interior, U.S. Geological Survey, http://edcftp.cr.usgs.gov/pub/data/DEM/250/, Cited: June 5, 2007.

[21] C.-Y. Wan, A. T. Campbell, and J. Crowcroft, "A case for all-wireless, dual-radio virtual sinks," in *SenSys '04: Proceedings of the 2nd international conference on Embedded networked sensor systems*. New York, NY, USA: ACM, 2004, pp. 267–268.

[22] C. Zhang, J. Kurose, Y. Liu, D. Towsley, and M. Zink, "A Distributed Algorithm for Joint Sensing and Routing in Wireless Networks with Non-Steerable Directional Antennas," in *Proceedings of the IEEE ICNP Conference, Santa Barbara, CA, USA*, Nov. 2006.